Global imaging of polar cap patches with dual airglow imagers

K. Hosokawa[1,2], S. Taguchi[1,2], K. Shiokawa[3], Y. Otsuka[3], Y. Ogawa[4] and M. Nicolls[5]

[1] Dept. of Comm. Eng. and Informatics, Univ. of Electro-Communications, Tokyo, Japan
[2] Center for Space Science and Radio Engineering, Univ. of Electro-Communications, Tokyo, Japan
[3] Solar-Terrestrial Environment Laboratory, Nagoya University, Nagoya, Japan
[4] National Institute of Polar Research, Tokyo, Japan
[5] SRI International, CA, USA

Correspondence

Keisuke Hosokawa
Dept. of Comm. Eng. and Informatics
University of Electro-Communications,
Tokyo 182-8585, Japan

Tel: +81 424 43 5299
Fax: +81 424 43 5293

Email: keisuke.hosokawa@uec.ac.jp

For submission to *Geophysical Research Letters*

Abstract. During a 2-h interval from 2240 to 2440 UT on November 12, 2012, regions of increased 630.0 nm airglow emission were simultaneously detected by dual all-sky imagers in the polar cap, one at Longyearbyen, Norway (78.1N, 15.5E) and the other at Resolute Bay, Canada (74.7N, 265.1E). The Resolute Bay incoherent scatter radar observed clear enhancements of the F region electron density up to 10^{12} m^{-3} within these airglow structures, which indicates that these are optical manifestations of polar cap patches propagating across the polar cap. During this interval of simultaneous airglow imaging, the nightside/dawnside (dayside/duskside) half of the patches was captured by the imager at Longyearbyen (Resolute Bay). This unique situation enabled us to estimate the dawn-dusk extent of the patches to be around 1500 km, which was at least 60–70% of the width of the anti-sunward plasma stream seen in the SuperDARN convection maps. In contrast to the large extent in the dawn-dusk direction, the noon-midnight thickness of each patch was less than 500 km. This means that there exists a class of polar cap patches whose shape shows significant anisotropy. From these observations, we conclude that patches can be produced not only in a localized area near the cusp but also in a wide range of local time on the dayside nearly simultaneously.

1. Introduction

Polar cap patches are chunks of dense plasma in the polar cap F region ionosphere whose horizontal extent typically ranges from 100 to 1000 km [*Crowley et al.*, 1996]. Patches are produced near the dayside cusp and transported towards the nightside along the anti-sunward plasma convection in the polar cap. Since the electron density within patches is often enhanced by a factor of 2–10 above the background level, airglow measurements at 630.0 nm wavelength are able to detect patches [*Weber et al.*, 1984]. During the last decade, a highly-sensitive all-sky airglow imager (ASI) of Optical Mesosphere Thermosphere Imagers (OMTIs) [*Shiokawa et al.*, 2009] at Resolute Bay, Canada (RSB; 74.7N, 265.1E, 82.9 MLAT) has been widely used to visualize the dynamical characteristics of patches in a two dimensional fashion [e.g., *Hosokawa et al.*, 2009; *Dahlgren et al.*, 2012]. However, the field-of-view (FOV) of a single ASI is not large enough to observe entire patches; thus, it has been rather difficult to discuss the distribution/shape/propagation of patches in a global context.

In order to image patches more globally, an additional ASI has been operative since October 2011 in Longyearbyen, Norway (LYR; 78.1N, 15.5E, 75.3 MLAT) [*Taguchi et al.*, 2012]. Since the deployment of this new imager, the polar cap ionosphere has been watched from two sites simultaneously. As one of the first results from the global imaging of the polar cap with dual ASIs, we present a patch event on November 12, 2012, during which patches were captured commonly by the two ASIs. We also employ an incoherent scatter radar at RSB (RISR-N, e.g., *Dahlgren et al.* [2012]) and Super Dual Auroral Radar Network (SuperDARN) to observe the electron density and plasma convection, respectively. By combining these data, we succeeded in monitoring the propagation of patches for ∼2 hours, which allows us to estimate the spatial extent of the patches from composite snapshot images. The derived large-scale structure of the patches is discussed in terms of the generation/propagation processes of high density plasma in the central polar cap region.

2. Observations

During a 4-h interval from 2100 to 2500 UT on November 12, 2012, a series of polar cap patches was observed by the two ASIs at RSB and LYR, and RISR-N. Figure 1a presents the temporal variation of the vertical electron density profile obtained from RISR-N in a format of altitude-time-intensity plot. The F region electron density was high in most of time, indicating that dense plasmas in the sunlit hemisphere were continuously delivered to the polar cap over RSB during this interval. In particular, several outstanding blobs of high density plasma were seen above 200 km altitudes, for example before 2140 UT, at around 2210 UT, and from 2330 to 2430 UT. The electron density within the blobs was as large as 10^{12} m^{-3}, which is a typical signature of polar cap patches in the incoherent scatter radar data.

Figure 1b shows the 630.0 nm ASI data from RSB in a format of keogram along the E–W cross section. When the ASI started its operation at 2240 UT, the FOV was located at $\sim$15 MLT; thus, the ASI at RSB mainly covered the dayside/duskside part of the polar cap during the present interval. A continuous bright region in the western edge of the keogram is contaminations of daylight. The ASI observed several traces appearing from the western edge and moving eastward through the zenith, which are manifestations of patches in keograms. Relatively brighter patches were detected from 2330 to 2430 UT, which is consistent with the appearance of dense plasma in the RISR-N data in this time period. Even before 2330 UT, a few faint patches appeared in the FOV of the ASI and their signatures can also be seen in the RISR-N data as slight increases in the F region electron density.

Figure 1c displays the 630.0 nm ASI data from LYR. The FOV of the ASI was situated at $\sim$02 MLT; thus, the ASI at LYR was mainly observing the nigthside/dawnside part of the polar cap. Here, we show the data as a keogram along the SW–NE cross section, which is a favorable direction for tracking the anti-sunward motion of the patches. A prominent structure near the SW edge of the keogram corresponds to the poleward edge of the auroral oval on the nightside. During the first half of the interval, say before 2250 UT, a number of bright patches were detected as slanted traces. These luminous patches should correspond to the blobs of dense plasma seen in the RISR-N data before 2215 UT. Unfortunately, the RSB ASI was not operative before 2240 UT; thus, there was no chance for global imaging in the first half of the interval. In contrast, a few weak traces of patches were observed by both ASIs from 2240 to 2420 UT which is marked by the green rectangle in the keograms. This is an interval of the global imaging of patches by dual ASIs. After ∼2330 UT, a large part of the FOV of the LYR ASI was filled with polar cap auroras which are predominant phenomena during the northward IMF conditions [e.g., *Hosokawa et al.*, 2011]. Such auroras made it difficult to observe polar cap patches from LYR, especially near the zenith.

Figures 1d–f respectively show the IMF B_y, IMF B_z, and solar wind V_x which were obtained from the ACE spacecraft located far upstream of the Earth (X_{GSM} ∼220 $\mathrm{R_E}$). An average V_x of ∼310 km s^{-1} and proton density of ∼40 cc^{-1} (not shown) were measured during the interval, implying a delay of ∼82 min between the spacecraft location and the dayside ionosphere [*Khan and Cowley*, 1999]. The time-series in Figures 1d–f have been shifted accordingly. The IMF B_y shown in Figure 1d was always positive ∼5 nT until around 2405 UT, and after that it was directed predominantly negative. The IMF B_z shown in Figure 1e was mostly negative until 2350 UT; thus, conditions were favorable for the generation of patches and their subsequent transportation towards the central polar cap. After 2350 UT, however, the B_z showed large-scale oscillations during which polar cap auroras appeared over LYR.

Figure 2 shows a sequence of composite 630.0 nm images every 20 min from 2240 to 2420 UT. Here, the original images have been mapped onto the MLAT/MLT coordinate system. As shown in Figure 2a, the RSB ASI covered the dayside/duskside part of the polar cap and the dayside half of the FOV was illuminated by the Sun. The red line within the RSB FOV shows the E–W cross section used in Figure 1b. The LYR ASI observed the nightside/dawnside part of the polar cap and prominent aurora was seen near the equatorward edge of the FOV. Overplotted with the blue line is the SW–NE cross section used in Figure 1c. It should be noted that the red and blue cross sections in Figure 2a are almost parallel to the anti-sunward motion of patches; thus, they are suitable for tracking their propagation process. At 2240 UT, there existed several regions of enhanced 630.0 nm emission in the poleward half of the FOVs of both ASIs. These are signatures of polar cap patches simultaneously captured by the dual ASIs.

At later times, the basic structures remained similar to those seen at 2240 UT. That is, the patches were streaming in the central polar cap, and the dayside/duskside (nightside/dawnside) half of the patches was captured by the ASI at RSB (LYR). At 2420 UT, for example, both ASIs observed patches which showed successive cigar-shaped structures elongating mainly in the dawn-dusk direction. This again confirms that the dual ASIs were detecting common patches during the 2-h interval, which would be a unique opportunity for imaging the spatial distribution of patches in a global context. An animation showing the temporal evolution of the patches during the interval at a rate of one frame every 2 min accompanies the electronic version of this article (Animation 1). The animation sequence more clearly demonstrates that the patches were captured by the two ASIs simultaneously and they were propagating anti-sunward through the FOVs of both ASIs.

In Figures 2b–e, contours of electrostatic potential derived from all the northern hemisphere SuperDARN radars using an algorithm developed by *Ruohoniemi and Baker* [1998] have been superimposed on the composite ASI images. In general, the potential contours show the typical twin cell convection pattern, and the plasma flow in the polar cap region has a small duskward component. This pattern is consistent with the prevailing positive IMF B_y and negative B_z during the present interval [e.g., *Hosokawa et al.*, 2009]. It is more clearly seen in Figures 2d and e that the stream of the patches was well aligned with the slightly tilted anti-sunward convection in the central polar cap. This implies that the dawn-dusk extent of patches has a close relationship with the width of the anti-sunward polar cap convection. We will discuss this point in the Discussion section.

3. Discussion and Summary

On November 12, 2012, simultaneous airglow measurements of polar cap patches were achieved from two separate sites in the polar cap region, which allows us to extract the spatial extent of patches from composite snapshot images. Figure 3a shows a picture composed of dual 630.0 nm images at 2306 UT. In the poleward portion of the FOVs, several dim regions of enhanced airglow are seen, which are signatures of patches streaming anti-sunward in the central polar cap. Here, the dawnside and duskside edges of the bright optical stream are outlined by the two dashed red lines, respectively. An approximate dawn-dusk extent of the stream (i.e., the separation between the dashed red lines in Figure 3a) ranges from 1500 to 2000 km. All the composite images in Figure 2 demonstrate similar scale size of patches in the dawn-dusk direction. It means that the dawn-dusk extent of the patch stream did not change very much during the interval of interest.

In Figure 3b, the high-latitude convection pattern derived from SuperDARN is superimposed on the airglow images. By comparing the optical data with the convection streamlines, the dawn-dusk extent of the patches is found to be at least 60–70% of the width of the anti-sunward flow in the polar cap. The other important point in Figure 3a is that the dawn-dusk extent of the patches is slightly larger on the nightside than that on the dayside. This tendency can also be seen in some of the panels in Figure 2. In any models of the high-latitude convection [e.g., *Ruohoniemi and Greenwald*, 2005], the streamlines of the polar cap flow tend to be relaxed on the nightside, i.e., the dawn-dusk width of the polar cap convection can be broader on the nightside. Such a relaxation of the anti-sunward flow could be responsible for the dawn-dusk elongation of patches in the polar cap. In the past studies, elongation of patches has been believed to occur after they exit the polar cap boundary on the nightside. *Robinson et al.* [1985] demonstrated that such elongation occurs when patches straddle convection streamlines that circulate in the sunward return flow in the dawn and dusk sectors. During the current interval, however, elongation occurred even in the polar cap, well before the patches entered the auroral region.

By using the composite image in Figure 3a, the extent of the patches in the direction of their motion can also be estimated. At the time of Figure 3a, three cigar-shaped patches were seen in the central polar cap. While the dawn-dusk extent of these patches was 1500–2000 km, the noon-midnight thickness of each patch was less than 500 km, which is indicated by the green lines in Figure 3a. This means that the spatial distribution of the patches was significantly anisotropic; the thickness of the patches is roughly 30% of their scale size in the dawn-dusk direction. In the past literature, *MacDougall and Jayachandran* [2007] derived a similar anisotropic shape of polar cap patches by calculating cross correlation analysis of the ionosonde data in the polar cap. More recently, *Hosokawa et al.* [2013] reported similar cigar-shaped patches propagating through the FOV of the LYR ASI successively. At that time, however, they could not estimate the dawn-dusk extent of the patches because their scale size in the direction of elongation was larger than the FOV of the ASI. Therefore, our imaging observation with dual ASIs directly confirms the anisotropic shape of patches for the first time.

In the past literature, the generation of polar cap patches has been observed mostly in a localized area near the dayside cusp. Thus, we might have believed that the production of patches occurs in a longitudinally narrow region along the dayside polar cap boundary. In the current interval, however, the dawn-dusk extent of the patches was found to be very large, 1500–2000 km. The simultaneous SuperDARN convection maps implied that their source should have extended over at least a few hours of MLT on the dayside (e.g., Figure 3b). Although there are many different generation processes of patches proposed so far [*Carlson et al.,* 2012 and references therein], most of them employed periodic flow bursts due to transient dayside reconnection as a process capturing the daytime high-density plasma into the polar cap as patches. The estimated large dawn-dusk extent of patches implies that a certain class of patches can be directly generated by such periodic flow bursts occurring across a wide range of MLT along the dayside polar cap boundary, for example as visualized by *Milan et al.* [2000]. In such a situation, patches have to show significant anisotropy in their shape when produced. After the generation of such patches, the relaxation of the anti-sunward convection plays an additional role in elongating them in the dawn-dusk direction, and consequently the patches are observed as a cigar-shaped structure in the central polar cap region.

It has been suggested that storm enhanced density (SED) is a source of polar cap patches during severely disturbed conditions like geomagnetic storms. SED is known as a narrow plume of high density plasma streaming from the daytime mid-latitude region towards the cusp inflow region [*Foster*, 1993]. *Foster et al.* [2005] demonstrated an existence of polar cap tongue of ionization (TOI) originating from an SED during a huge storm in November 2003. The cross-plume width of TOI was as large as 800 km, which is narrower than the dawn-dusk extent of the patches during the present interval. More recently, *Hosokawa et al.* [2010] observed a large-scale optical signature of TOI extending from an SED during a large magnetic storm on December 15, 2006. In their event, the dawn-dusk extent of the optical plume was 300–500 km, which is again much narrower than that of the patches during the current period. They also demonstrated that the plume was seen in a limited part of the anti-sunward convection in the polar cap. These observations suggest that the dawn-dusk extent of patches/TOIs during magnetic storms could be narrower than that during moderately disturbed conditions. This is possibly because the source of storm time patches (i.e., SED) is already confined in longitude before the anti-sunward flow entrains the source plasmas further into the polar cap. That is, the spatial distribution of propagating high density plasma in the polar cap can be different depending on the geomagnetic activity. Such a characteristic could be an important key knowledge for better predicting the space weather impact of streaming high density plasma in the polar cap region.

Acknowledgments. We would like to thank Takeshi Aoki for his continuous support for making/installing/maintaining our optical instrument in Longyearbyen. This work was supported by Grants-in-Aid for Scientific Research (22340143, 23740366 and 20244080) from the Japan Society for the Promotion of Science (JSPS). This work was carried out by the joint research program of the Solar-Terrestrial Environment Laboratory (STEL), Nagoya University. The optical observation at Resolute Bay was also supported by the NSF cooperative agreement ATM-0608577. The authors wish to thank N. Ness at the Bartol Research Institute for access to data from MFI and SWE instruments onboard the ACE spacecraft.

References

Crowley, G. (1996), Critical review of ionospheric patches and blobs, in *Review of Radio Science 1993-1996*, edited by W. R. Stone, Oxford University Press, New York, 619.

Dahlgren, H., J. L. Semeter, K. Hosokawa, M. J. Nicolls, T. W. Butler, M. G. Johnsen, K. Shiokawa, and C. Heinselman (2012), Direct three-dimensional imaging of polar ionospheric structures with the Resolute Bay Incoherent Scatter Radar, *Geophys. Res. Lett., 39*, doi:10.1029/2012GL050895.

Foster, J. C. (1993), Storm-time plasma transport at middle and high latitudes, *J. Geophys. Res., 98*, 1675.

Foster, J. C., et al. (2005), Multiradar observations of the polar tongue of ionization, *J. Geophys. Res., 110*, doi:10.1029/2004JA010928.

Hosokawa, K., T. Kashimoto, S. Suzuki, K. Shiokawa, Y. Otsuka and T. Ogawa (2009), Motion of polar cap patches: A statistical study with all-sky airglow imager at Resolute Bay, Canada, *J. Geophys. Res., 114*, 10.1029/2008JA014020.

Hosokawa, K., T. Tsugawa, K. Shiokawa, Y. Otsuka, N. Nishitani, T. Ogawa, and M. R. Hairston (2010), Dynamic temporal evolution of polar cap tongue of ionization during magnetic storm, *J. Geophys. Res., 115*, doi:10.1029/2010JA015848.

Hosokawa, K., J. I. Moen, K. Shiokawa, and Y. Otsuka (2011), Motion of polar cap arcs, *J. Geophys.*

Res., 116, doi:10.1029/2010JA015906, 2011.

Hosokawa K., S. Taguchi, Y. Ogawa, and T. Aoki, (2013), Periodicities of polar cap patches, *J. Geophys. Res., 118*, doi:10.1029/2012JA018165.

Khan, H., S. W. H. Cowley (1999), Observations of the response time of high-latitude ionospheric convection to variations in the interplanetary magnetic field using EISCAT and IMP-8 data, *Ann. Geophys., 17*, 1306.

MacDougall J., P. T. Jayachandran (2007), Polar patches: Auroral zone precipitation effects, *J. Geophys. Res., 112*, doi:10.1029/2006JA011930.

Milan, S., M. Lester, S. Cowley, and M. Brittnacher (2000), Convection and auroral response to a southward turning of the IMF: Polar UVI, CUTLASS, and IMAGE signatures of transient magnetic flux transfer at the magnetopause, *J. Geophys. Res., 105*, 15,741.

Oksavik, K., V. L. Barth, J. Moen, and M. Lester (2010), On the entry and transit of high-density plasma across the polar cap, *J. Geophys. Res., 115*, doi:10.1029/2010JA015817.

Robinson, R. M., R. T. Tsunoda, J. F. Vickrey, and L. Guerin (1985), Sources of F Region Ionization Enhancements in the Nighttime Auroral Zone, *J. Geophys. Res., 90*, 7533.

Ruohoniemi, J., and K. Baker (1998), Large-scale imaging of high-latitude convection with Super Dual Auroral Radar Network HF radar observations, *J. Geophys. Res., 103*, 20,797.

Ruohoniemi, J. M., and R. A. Greenwald (2005), Dependencies of high-latitude plasma convection: Consideration of interplanetary magnetic field, seasonal, and universal time factors in statistical patterns, *J. Geophys. Res., 110*, 10.1029/2004JA010815.

Shiokawa, K., Y. Otsuka, and T. Ogawa (2009), Propagation characteristics of nighttime mesospheric and thermospheric waves observed by optical mesosphere thermosphere imagers at middle and low latitudes, *Earth Planets Space, 61*, 479.

Taguchi, S., K. Hosokawa, Y. Ogawa, T. Aoki, and M. Taguchi (2012), Double bursts inside a poleward-moving auroral form in the cusp, *J. Geophys. Res., 117*, doi:10.1029/2012JA018150.

Weber, E. J., J. Buchau, J. G. Moore, J. R. Sharber, R. C. Livingston, J. D. Winningham, and B. W. Reinisch (1984), F layer ionization patches in the polar caps, *J. Geophys. Res., 89*, 1683.

Figure Captions

Figure 1 (a) Altitude-Time-Intensity plot of the electron density obtained along the vertical beam (beam ID 65486) of RISR-N during a 4-h interval from 2100 to 2500 UT on November 12, 2012 (b) Keogram reproduced from 630.0 nm all-sky images from Resolute Bay along the E—W cross section (c) Keogram reproduced from 630.0 nm all-sky images from Longyearbyen along the SW–NE cross section (d–f) IMF B_y, IMF B_y and solar wind V_x obtained from the ACE spacecraft. The time-series is shifted by 82 min to account for the solar wind propagation delay from the spacecraft to the dayside polar cap.

Figure 2 Sequence of composite 630.0 nm airglow images obtained from the two sites at $\sim$20 min intervals from 2240 to 2420 UT. In the panels b–e, the SuperDARN map potential contours are superimposed on the ASI images.

Figure 3 (a) Snapshot of composite 630.0 nm airglow images at 2306 UT. (b) Same as (a), but the SuperDARN map potential contours and estimated velocity vectors are superimposed.

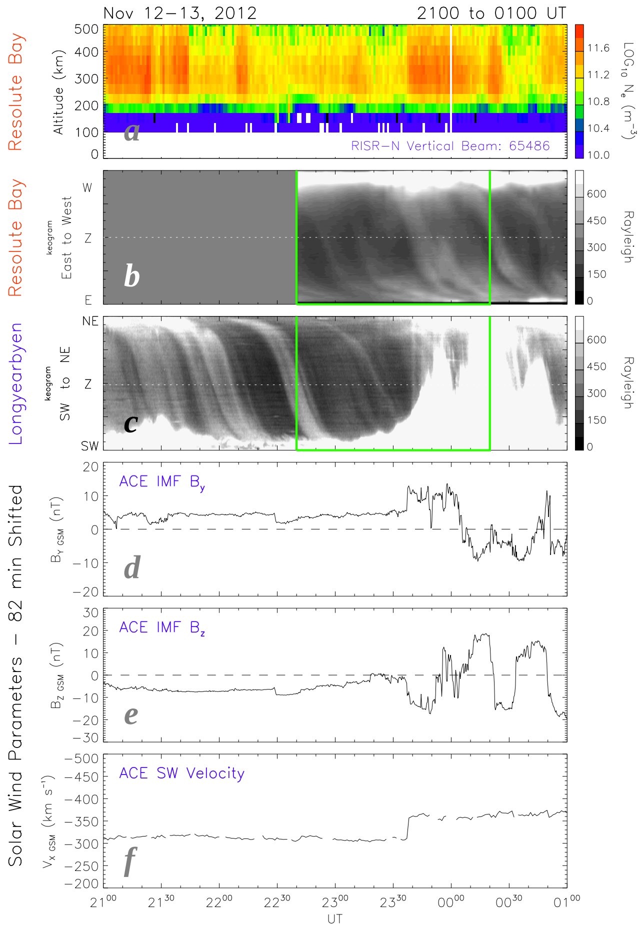

Figure 1

Figure 1 (a) Altitude-Time-Intensity plot of the electron density obtained along the vertical beam (beam ID 65486) of RISR-N during a 4-h interval from 2100 to 2500 UT on November 12, 2012 (b) Keogram reproduced from 630.0 nm all-sky images from Resolute Bay along the E—W cross section (c) Keogram reproduced from 630.0 nm all-sky images from Longyearbyen along the SW–NE cross section (d–f) IMF B_y, IMF B_y and solar wind V_x obtained from the ACE spacecraft. The time-series is shifted by 82 min to account for the solar wind propagation delay from the spacecraft to the dayside polar cap.

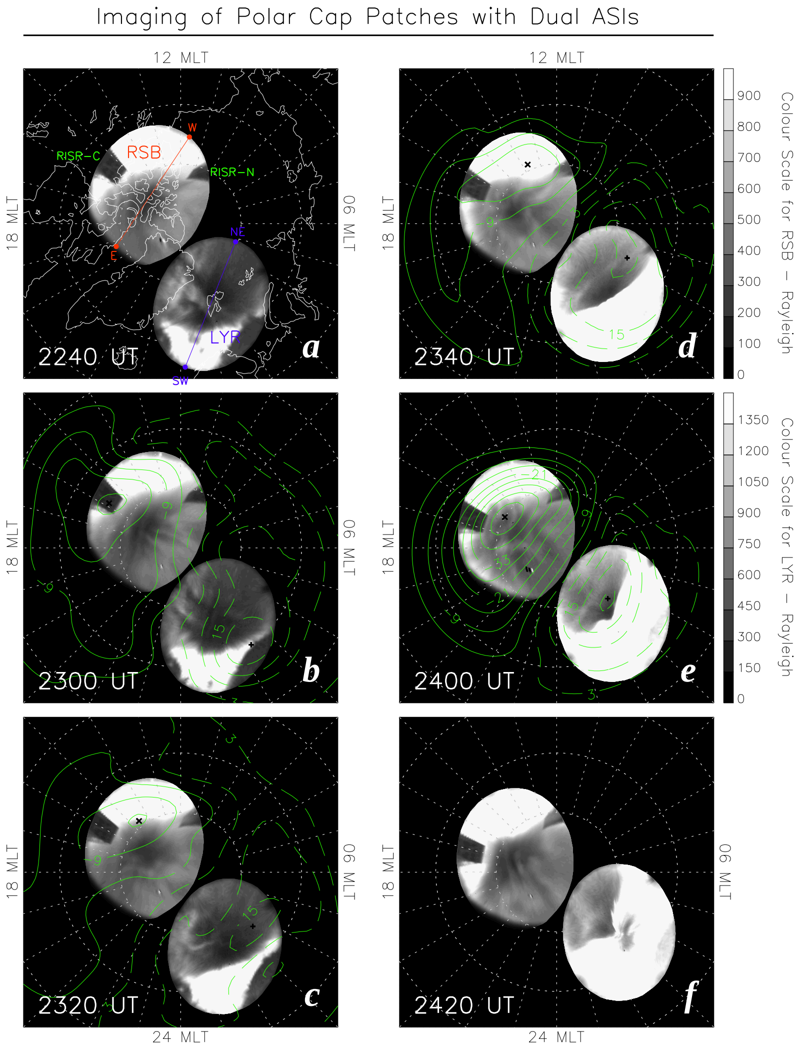

Figure 2

Figure 2 Sequence of composite 630.0 nm airglow images obtained from the two sites at ∼20 min intervals from 2240 to 2420 UT. In the panels b–e, the SuperDARN map potential contours are superimposed on the ASI images.

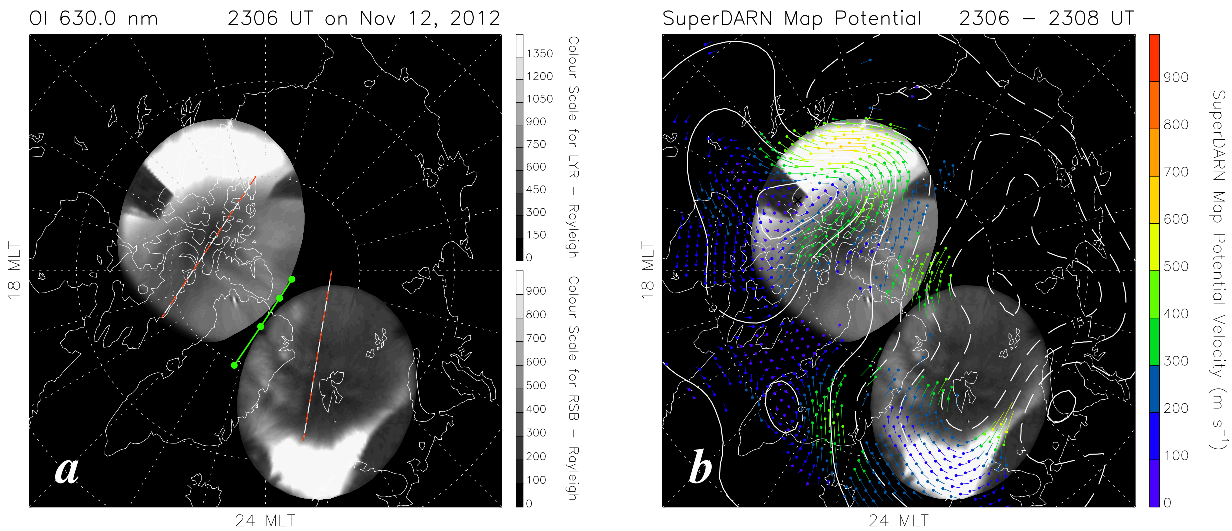

Figure 3

Figure 3 (a) Snapshot of composite 630.0 nm airglow images at 2306 UT. (b) Same as (a), but the SuperDARN map potential contours and estimated velocity vectors are superimposed.